Journal of the Optical Society of America A
OPTICS, IMAGE SCIENCE, AND VISION

Does the quasi-static polarizability have principal axes?

VADIM A. MARKEL

Department of Radiology, University of Pennsylvania, Philadelphia, Pennsylvania 19104, USA (vmarkel@upenn.edu)

Received 11 March 2024; revised 10 May 2024; accepted 14 May 2024; posted 14 May 2024; published 7 June 2024

Beyond strict statics, the dipole polarizability tensor is a complex symmetric matrix. Such matrices may not be diagonalizable by an orthogonal similarity transformation (a rigid rotation of the reference frame). In this paper, we provide examples of polarizability tensors that have no real principal axes and discuss the conditions under which this counter-intuitive phenomenon can occur.

https://doi.org/10.1364/JOSAA.523449

1. INTRODUCTION

The quasi-static dipole polarizability plays an important role in the theory of electromagnetic scattering. In the Rayleigh limit when the wavelength of the incident light is assumed to be infinite, the extinction and scattering cross sections of a non-magnetic particle are given (in the Gaussian system of units, which is used throughout the paper) by the expressions

$$\sigma_e = \frac{4\pi k}{|\mathbf{E}_0|^2}\mathrm{Im}[\mathbf{E}_0^* \cdot \hat{\alpha}\mathbf{E}_0], \quad \sigma_s = \frac{8\pi k^4}{3|\mathbf{E}_0|^2}\mathbf{E}_0^* \cdot (\hat{\alpha}^*\hat{\alpha})\mathbf{E}_0\,. \quad (1)$$

These formulas are written for a (quasi)-monochromatic incident plane wave of the complex amplitude $\mathbf{E}_0$, $k = \omega/c$ is the wave number at the central frequency ω, and $\hat{\alpha}$ is the quasi-static electric dipole polarizability tensor evaluated at the same frequency. The star in $\hat{\alpha}^*$ denotes element-wise complex conjugation. The expressions in Eq. (1) are well known and appear in various forms in many textbooks; generalizations to non-monochromatic light in an arbitrary state of polarization are also known [1]. The purpose of this paper is to point out that, contrary to common wisdom, $\hat{\alpha}$ is not always diagonalizable by an orthogonal similarity transformation, i.e., by rotation of the reference frame. In other words, a Cartesian reference frame XYZ in which $\hat{\alpha}$ is diagonal may not exist. One physical implication of this observation is that some particles can never be at equilibrium when illuminated by a plane wave but always experience a nonzero torque. This can create an additional mechanism for energy dissipation.

In spite of its significance, the question of whether $\hat{\alpha}$ has real principal axes is almost never addressed in the textbooks or even in the specialized literature. There appear to be two main reasons for this omission. First, it is true that, at zero frequency, $\hat{\alpha}$ is a real symmetric matrix and therefore is diagonal in some real principal axes. However, beyond strict statics, $\hat{\alpha}$ is complex symmetric and there is no mathematical guarantee that its eigenvectors are real. It may not even have three linearly independent eigenvectors (such matrices are called *defective*). Even if $\hat{\alpha}$ is not defective, its eigenvectors can be complex and not reducible to real vectors by multiplication with a constant. Such vectors do not have a direction and do not correspond to any geometrical axes in the physical space. The second reason is that the particles considered in the scattering theory often have special symmetries that force $\hat{\alpha}$ to be diagonalizable in real axes even if its elements are complex. Examples of such particles include spheres, ellipsoids, cuboids, truncated cylinders, cones, toruses, and many other regular shapes. It may seem that, since in all these cases the complexity of $\hat{\alpha}$ does not prevent it from having real principal axes, the property is general and we just did not yet find its mathematical proof. However, we will demonstrate below that the property is not general and can break down quite dramatically in some cases.

The rest of this paper is organized as follows. In Section 2 we explain the physical model used to compute $\hat{\alpha}$. We then provide in Section 3 a couple of numerical examples in which $\hat{\alpha}$ is not diagonalizable in real axes. Finally, Section 4 contains a discussion.

2. MODEL

To provide counter-examples illustrating the main point of this paper, we need to compute $\hat{\alpha}$ for particles of complicated shape and without any special symmetries. We will adopt to this end the coupled-dipole model. Specifically, we will construct an aggregated particle whose polarizability $\hat{\alpha}$ we want to compute from N equivalent point-like particles whose polarizability $\hat{\alpha}_0$ is known and simple. Then $\hat{\alpha}$ can be found by solving a set of $3N$ linear equations. We do not assume that this set of point particles mimics in any way a continuous particle. Consequently, our model is different from the discrete-dipole approximation (DDA) [2,3]. Rather, we assume that there is a collection of rigidly connected point-like polarizable particles with some physically reasonable properties and that these particles can

interact with each other and the external field. We can visualize this system as a collection of several small spheres with known dielectric permittivity ϵ. This physical interpretation is convenient and will be used below (we always place the elementary spheres sufficiently far apart for the dipole approximation to be accurate), but it is not the only possible interpretation. A recent review of the coupled-dipole model as applied to a general collection of particles can be found in [4], and a review focused more specifically on the DDA in [5].

Let us assume that a set of points $\mathbf{r}_i$, $i = 1, ..., N$, has been generated by some method. We associate with each point an elementary sphere of radius a made from a conductor with the Drude complex permittivity

$$\epsilon(\omega) = 1 - \frac{\omega_p^2}{\omega(\omega + \mathrm{i}\gamma)}, \tag{2}$$

where ω_p is the plasma frequency and γ is the relaxation constant. The dipole polarizability of each elementary sphere is

$$\hat{\alpha}_0(\omega) = a^3 \frac{\epsilon(\omega) - 1}{\epsilon(\omega) + 2} \hat{I}, \tag{3}$$

where $\hat{I}$ is the identity tensor. If the system is placed in the external electric field $\mathbf{E}(t) = \mathrm{Re}[\mathbf{E}_0 e^{-\mathrm{i}\omega t}]$, the dipole moments induced in each elementary sphere would satisfy the coupled-dipole equation

$$\kappa(\omega)\mathbf{d}_i = a^3 \mathbf{E}_0 + \sum_{j=1, j\neq i}^{N} a^3 \hat{G}(\mathbf{r}_i, \mathbf{r}_j)\mathbf{d}_j, \tag{4}$$

where

$$\kappa(\omega) = 1 - (\omega/\omega_F)^2 - \mathrm{i}(\gamma\omega/\omega_F^2). \tag{5}$$

Here $\hat{G}(\mathbf{r}_i, \mathbf{r}_j)$ is the static limit of the Green's tensor for the electric field (e.g., given in Eq. 4.13b of [6]) and $\omega_F = \omega_p/\sqrt{3}$ is the Frohlich frequency. We have used Eqs. (2) and (3) to arrive at expression (5) for $\kappa(\omega)$. Given the external field amplitude $\mathbf{E}_0$ and the frequency ω, we can solve Eq. (4) and find the elementary dipole moments $\mathbf{d}_i$. The cumulative dipole moment of the aggregate is simply the direct sum of the former quantities:

$$\mathbf{D} = \sum_{i=1}^{N} \mathbf{d}_i. \tag{6}$$

Once $\mathbf{D}$ is found, we can compute $\hat{\alpha}$ from the relation $\mathbf{D} = \hat{\alpha}\mathbf{E}_0$. To find all six independent elements of $\hat{\alpha}$, we can solve Eq. (4) with three different right-hand sides, taking consecutively $\mathbf{E}_0 = \hat{\boldsymbol{x}}$, $\mathbf{E}_0 = \hat{\boldsymbol{y}}$, and $\mathbf{E}_0 = \hat{\boldsymbol{z}}$.

3. NUMERICAL EXAMPLES

Our first numerical example was obtained for the aggregate of elementary spheres of the radius $a = 0.25$ shown in Fig. 1. To generate the aggregate, we have placed $N = 73$ points $\mathbf{r}_i$ randomly inside a sphere of the radius $R = 2.5$ and centered at the origin. The points were not allowed to approach each other closer than the distance 1.0 so that all pair-wise distances satisfy $|\mathbf{r}_i - \mathbf{r}_j| > 1.0$. Consequently, all surface-to-surface distances

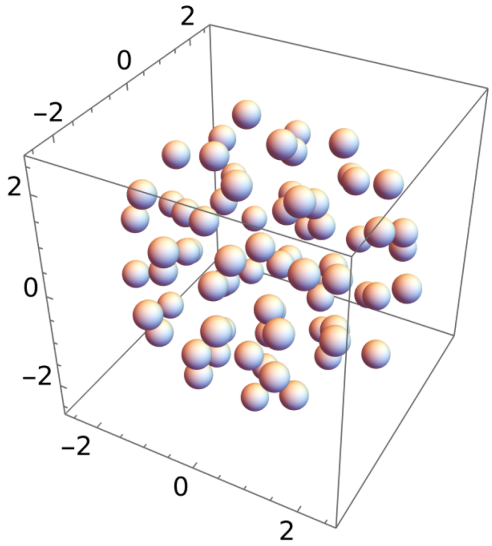

Fig. 1. Aggregate of $N = 73$ spherical particles of radius $a = 0.25$ each. Center-to-center distance between any two particles is larger than $4a = 1.0$. Centers of all particles are contained in a sphere of the radius $R = 2.5$ centered at the origin. In the quasi-static approximation, the physical units in which the lengths are measured are unimportant.

between any two elementary spheres are greater than one sphere diameter. The volume fill fraction of the elementary spheres inside the large sphere is approximately 0.073 (not accounting for the boundary effects), which is much smaller than the theoretical maximum of 0.65 for random packing. We emphasize that, in quasi-statics, the physical units in which the distances are measured are unimportant [7].

Extinction spectra of the aggregate are shown in Fig. 2 for $\mathbf{E}_0 = \hat{\boldsymbol{x}}$, $0.94 \le \omega/\omega_F \le 1.06$ (this is the spectral region where the electromagnetic resonances of the aggregate are supported), and different ratios γ/ω_p. The dimensionless specific extinction plotted in the figure is defined as

$$Q = \frac{\sigma_e}{kV}, \quad V = N\frac{4\pi a^3}{3}, \tag{7}$$

where V is the total volume of the elementary spheres. The extinction cross section σ_e can be computed using the polarizability tensor of the aggregate $\hat{\alpha}$ and the first formula in Eq. (1) or using the elementary dipoles $\mathbf{d}_i$, viz.,

$$\sigma_e = \frac{4\pi k}{|\mathbf{E}_0|^2} \mathrm{Im} \sum_{i=1}^{N} \mathbf{E}_0^* \cdot \mathbf{d}_i. \tag{8}$$

Note that the wave number k cancels out of the expression for Q and therefore Q is independent of the physical dimensions of the aggregate, as long as the quasi-static approximation is applicable and all geometrical proportions are fixed. The ratios $\gamma/\omega_p = 0.2$ [Fig. 2(a)] and $\gamma/\omega_p = 0.02$ [Fig. 2(b)] are typical for poor to good conductors, and $\gamma/\omega = 0.002$ [Fig. 2(c)] is characteristic of silver. Smaller values of this parameter are unrealistic. In all three panels, we compare the spectrum of the aggregate to that of a single isolated sphere. It can be seen that, at $\gamma/\omega_p = 0.2$, the two spectra are indistinguishable (and fairly flat in the spectral region considered), which indicates that the electromagnetic interaction of the elementary spheres

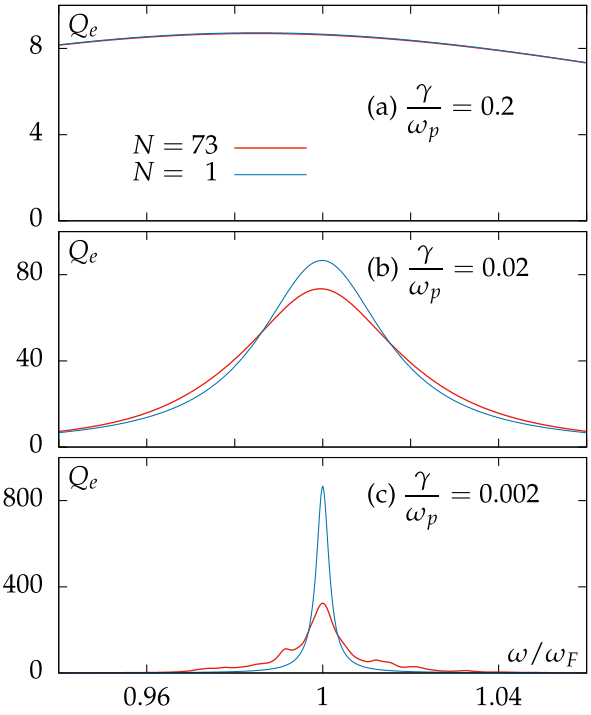

Fig. 2. Extinction spectra of the aggregate shown in Fig. 1 ($N = 73$) for different ratios of γ/ω_p compared to the spectrum of a single isolated sphere ($N = 1$). The extinction efficiency Q is defined in Eq. (7). The spectra were computed for X-polarization of the incident field, $\mathbf{E}_0 = \hat{\boldsymbol{x}}$, and are qualitatively similar in the other two polarizations.

in this case is negligible. At $\gamma/\omega_p = 0.02$, the spectrum of the aggregate is moderately broadened but is still quite smooth. At $\gamma/\omega_p = 0.002$, the spectrum is further broadened by the interaction and we start seeing the traces of individual resonances. Theoretically, there are $3N = 219$ such resonances in the system, but some of them can have zero or relatively small oscillator strengths and do not contribute to the spectrum noticeably.

Next, at each frequency ω that was considered in Fig. 2, we have computed the polarizability of the aggregate $\hat{\alpha}$ and its complex eigenvectors and eigenvalues $\mathbf{u}_p$ and α_p defined as

$$\hat{\alpha}\mathbf{u}_p = \alpha_p \mathbf{u}_p, \quad p = 1, 2, 3. \tag{9}$$

The eigenvectors have been normalized according to $\mathbf{u}_p^* \cdot \mathbf{u}_p = 1$ but are not orthogonal in the usual sense, so that, in general, $\mathbf{u}_p^* \cdot \mathbf{u}_q \neq \delta_{pq}$. Instead, eigenvectors of a complex symmetric matrix are orthogonal with respect to the dot product without complex conjugation, that is,

$$\mathbf{u}_p \cdot \mathbf{u}_q = Z_p \delta_{pq}, \quad p, q = 1, 2, 3. \tag{10}$$

The complex numbers Z_p are the squared pseudo-Euclidean norms of $\mathbf{u}_p$, $\|\mathbf{u}_p\|^2 = Z_p$. It is possible that a nonzero vector $\mathbf{u}_p \neq 0$ has a zero pseudo-Euclidean norm. A simple example is (1, i, 0). Such vectors are said to be quasi-null. In the case of complex symmetric matrices, the eigenvector associated with a defective eigenvalue is always quasi-null. For this and additional properties of complex symmetric matrices, see [8]. While matrix deficiency is an exotic property, the occurrence of $|Z_p| < 1$ is rather typical and signifies that the eigenvector $\mathbf{u}_p$ does not have a well-defined direction in the physical space. Such vectors

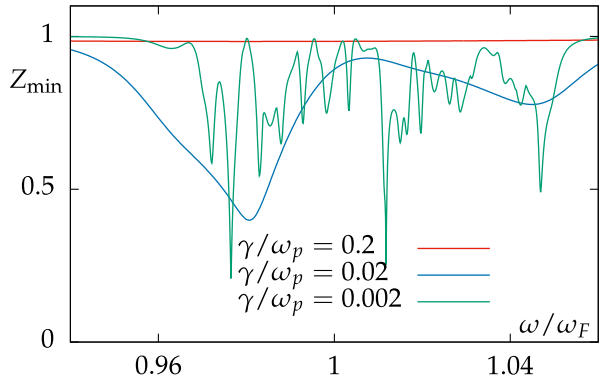

Fig. 3. Minimum pseudo-Euclidean norm of the eigenvectors of $\hat{\alpha}$, $Z_{\min}$ [defined in Eq. (11)], for the aggregate shown in Fig. 1 and same parameters as were used to compute the spectra in Fig. 2.

have complex components and cannot be transformed into purely real vectors by multiplication with any complex constant. If some of the eigenvectors of a non-degenerate matrix have $|Z_p| < 1$, the matrix cannot be diagonalized in purely real orthogonal principal axes.

In Fig. 3, we plot as a function of frequency the minimum absolute value of the pseudo-Euclidean norms of all three eigenvectors of $\hat{\alpha}$, viz.,

$$Z_{\min} := \min(|Z_1|, |Z_2|, |Z_3|)\,. \tag{11}$$

For $\gamma/\omega_p = 0.2$, $Z_{\min} \approx 1$ and the effect we wish to demonstrate is suppressed. However, for $\gamma/\omega_p = 0.02$ and $\gamma/\omega_p = 0.002$, the effect is quite visible. As a specific example, we summarize in Table 1 the algebraic properties of the matrix $\hat{\alpha}$ computed at $\omega/\omega_F = 0.97624$ for $\gamma/\omega_p = 0.002$. It can be seen that the matrix is non-degenerate and has three linearly independent, complex eigenvectors. Since all Z_p are non-zero, we can write

$$\hat{\alpha} = \sum_{p=1}^{3} Z_p^{-1} \alpha_p \mathbf{u}_p \mathbf{u}_p^T, \tag{12}$$

where the superscript T denotes transposition. We note that the eigenvalues in Table 1 are close but not the same; the difference is larger than the machine precision by many orders of magnitude. In fact, we expect $\hat{\alpha}$ to be quasi-isotropic as the aggregate was generated by a randomized algorithm that involves no preferred direction in space. In the limit $N \to \infty$, the aggregate is expected to be isotropic and similar to a sphere, with a degenerate $\hat{\alpha}$. However, the number of elementary spheres we have used ($N = 73$) is not large enough to achieve the thermodynamic limit. An intermediate conclusion is that the effect is present and can be quite strong in particles that are not too far from spheres but have broken symmetry with respect to any plane or axis, e.g., due to defects. Quasi-random aggregates such as the one shown in Fig. 1 satisfy this condition.

We have performed additional simulations in which spheres in Fig. 1 were replaced by randomly oriented spheroids (data not shown). The depolarization factors of the spheroids for the polarization along the axis of symmetry were taken to be $\nu_\parallel = 0.25$ (prolate spheroids) and $\nu_\parallel = 0.4$ (oblate spheroids). Qualitatively similar results to those shown in Fig. 3 were

Table 1. Algebraic Properties of the Cumulative Polarizability Computed for the Aggregate Shown in Fig. 1[a]

Polarizability tensor $\hat{\alpha}$

	x	y	z
x	(24.98, 8.61)	(-1.08, 0.65)	(-0.72, -0.65)
y	(-1.08, 0.65)	(27.12, 6.01)	(0.98, 0.06)
z	(-0.72, -0.65)	(0.98, 0.06)	(27.18, 7.89)

Eigenvalues α_p and eigenvectors $\mathbf{u}_p$

	$p=1$	$p=2$	$p=3$
α_p	(24.66, 8.60)	(27.72, 7.19)	(26.90, 6.73)
u_{px}	(0.91, 0.00)	(-0.16, 0.04)	(-0.11, -0.00)
u_{py}	(0.35, 0.03)	(0.23, -0.62)	(0.73, 0.00)
u_{pz}	(0.06, 0.23)	(0.74, 0.00)	(-0.25, 0.62)

Pseudo-Euclidean orthogonality table, $\mathbf{u}_p \cdot \mathbf{u}_q$

	$q=1$	$q=2$	$q=3$
$p=1$	(0.89, 0.05)	(0.00, 0.00)	(0.00, 0.00)
$p=2$	(0.00, 0.00)	(0.23, -0.29)	(0.00, 0.00)
$p=3$	(0.00, 0.00)	(0.00, 0.00)	(0.23, -0.31)

[a]The cumulative polarizability $\hat{\alpha}$ was computed for $\gamma/\omega_p = 0.002$ and $\omega/\omega_F = 0.97624$. All numbers in the tables have been rounded off to two figures after the decimal point. Complex numbers $z = x + iy$ are shown as (x, y). Zero values for $\mathbf{u}_p \cdot \mathbf{u}_q$ with $p \neq q$ have been computed with machine precision (about 15 figures after decimal point). Diagonal elements in the orthogonality matrix are the squared pseudo-Euclidean norms Z_p.

obtained with a somewhat stronger effect, with $Z_{\min} < 0.2$ for some frequencies in the case of oblate spheroids. Note that, within the coupled-dipole model, nonsphericity of particles provides an additional degree of freedom that can be used to break symmetries of the aggregate.

To gain more insight into the nature of the phenomenon, it is useful to utilize the spectral theory of polarizability developed by us in [9]. We re-write the coupled-dipole equation (4) in the matrix form as

$$\kappa(\omega)|\mathtt{d}\rangle = a^3|\mathtt{E}_0\rangle + \mathtt{W}\,|\mathtt{d}\rangle, \tag{13}$$

where we have used the typewrite-style font to denote $3N$-dimensional vectors and matrices. Thus, $|\mathtt{d}\rangle = (\mathbf{d}_1, \ldots, \mathbf{d}_N)^T$, $\mathtt{W}$ is a $3N \times 3N$ matrix built of the 3×3 dimensionless blocks $a^3\hat{G}(\mathbf{r}_i, \mathbf{r}_j)$, etc. What is important for us is that, in quasi-statics, the matrix $\mathtt{W}$ is real symmetric and therefore its eigenvectors and eigenvalues defined as

$$\mathtt{W}|\mathtt{d}_n\rangle = w_n|\mathtt{d}_n\rangle, \quad n = 1, \ldots, N \tag{14}$$

are real. In addition, the eigenvectors are orthonormal, $\langle\mathtt{d}_n|\mathtt{d}_m\rangle = \delta_{nm}$. We can utilize the orthogonality to write the solution to Eq. (13) in the form

$$|\mathtt{d}\rangle = a^3 \sum_{n=1}^{N} \frac{|\mathtt{d}_n\rangle\langle\mathtt{d}_n|\mathtt{E}_0\rangle}{\kappa(\omega) - w_n}. \tag{15}$$

The polarizability of the aggregate is then defined as

$$\alpha_{pq}(\omega) = a^3 \sum_{n=1}^{N} \frac{\langle\mathtt{O}_p|\mathtt{d}_n\rangle\langle\mathtt{d}_n|\mathtt{O}_q\rangle}{\kappa(\omega) - w_n}, \quad p, q = 1, 2, 3, \tag{16}$$

where $|\mathtt{O}_p\rangle$ has 1s in the positions $3(i-1)+p$ (for $i = 1, \ldots, N$) and 0s elsewhere. The eigenvalues w_n are supported in an interval of the real axis containing zero (we have trivially $\sum_n w_n = 0$). For the aggregate shown in Fig. 1, accounting for $a = 0.25$, we have $w_n \in [w_{\min}, w_{\max}]$, where $w_{\min} \approx -0.1$ and $w_{\max} \approx 0.06$. Writing $\omega/\omega_F = 1 + \delta$ and using Eq. (5), it is easy to see that the resonances in Eq. (16) (that is, the values of ω for which $\mathrm{Re}[\kappa(\omega)] = w_n$) can occur, approximately, in the interval $0.97 < \omega/\omega_F < 1.05$. A slightly larger spectral interval is shown in Figs. 2 and 3. If ω is far outside of this interval, or if $\mathrm{Im}[\kappa(\omega)] \gg w_{\max}$, we can neglect w_n in the denominator of Eq. (16). The summation then collapses to $\delta_{pq}a^3\kappa^{-1}(\omega)$, which is equivalent to the polarizability of an isolated sphere. The effect in this case is obviously absent.

Thus, we need resonances in order to obtain a non-diagonalizable (in real axes) $\hat{\alpha}$. However, the resonances should not be too strong. Indeed, consider the case when $\mathrm{Im}[\kappa(\omega)]$ is small, $\mathrm{Re}[\kappa(\omega)]$ is close to one of the eigenvalues w_m, and there are no other eigenvalues in a sufficiently large vicinity of w_m. Then we can neglect all the terms in Eq. (16) with $n \neq m$ to obtain

$$\alpha_{pq}(\omega) \approx \frac{a^3}{\kappa(\omega) - w_m}\langle\mathtt{O}_p|\mathtt{d}_m\rangle\langle\mathtt{d}_m|\mathtt{O}_q\rangle. \tag{17}$$

In this expression, $a^3/[\kappa(\omega) - w_m]$ is a complex scalar coefficient and $\langle\mathtt{O}_p|\mathtt{d}_m\rangle\langle\mathtt{d}_m|\mathtt{O}_q\rangle$ is a real symmetric 3×3 matrix. Clearly, $\hat{\alpha}(\omega)$ given by Eq. (17) has real orthogonal eigenvectors. Therefore, an essential requirement for observing the effect is spectral overlap of several strong resonances. When resonances become too narrow to overlap, the effect disappears. Indeed, for the aggregate shown in Fig. 1 and $\gamma/\omega_p = 10^{-6}$, we have $Z_{min}(\omega) > 0.97$ for all frequencies, so that the effect is negligible (data not shown).

Of course, $\gamma/\omega_p = 10^{-6}$ is unrealistically small. We can, however, illustrate suppression of the effect due to isolated resonances at realistic values of γ/ω_p in an aggregate with a smaller number of elementary spheres since in this case the eigenvalues w_n are not as densely packed. Consider the aggregate with $N = 4$ shown graphically in Fig. 4. The extinction spectra of this aggregate are plotted in Fig. 5. The ratio $\gamma/\omega_p = 0.2$ still corresponds to negligibly weak interaction, and the corresponding curve is not shown. In the case $\gamma/\omega_p = 0.02$, there is a strong interaction and a strong spectral overlap of all resonances, whereas, at $\gamma/\omega_p = 0.002$, the resonances are strong but the overlaps are weak. The spectral dependence of $Z_{\min}$ for this aggregate is shown in Fig. 6. The effect is not as strong as in the quasi-random aggregate with $N = 74$, but is still noticeable; $Z_{\min}$ can become as small as 0.86. It is also obvious that, at $\gamma/\omega_p = 0.002$, the effect is suppressed compared to the case $\gamma/\omega_p = 0.02$.

We finally adduce a summary of the algebraic properties of $\hat{\alpha}$ for the case $N = 4$ at $\gamma/\omega_p = 0.02$ and $\omega/\omega_F = 0.98812$ (close to the spectral minimum of $Z_{\min}$). The data are displayed in Table 2. One observation is that the aggregate is far from being isotropic; all three eigenvalues of $\hat{\alpha}$ are substantially different. Secondly, the aggregate has one real principal axis, $\mathbf{u}_2 = (-\sqrt{2}, 0, \sqrt{2})$. The other two eigenvectors are complex, with the (squared) pseudo-Euclidean norms $Z_1 = 0.72 + 0.47\mathrm{i}$ and $Z_3 = 0.76 - 0.41\mathrm{i}$ being quite far from unity.

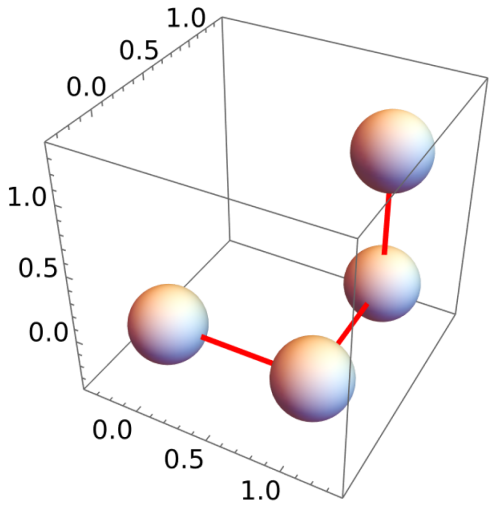

Fig. 4. Aggregate of $N=4$ spherical particles of radius $a=0.25$ each. Coordinates of the sphere centers are (0,0,0), (1,0,0), (1,1,0), and (1,1,1). Connecting lines are shown to guide the eye.

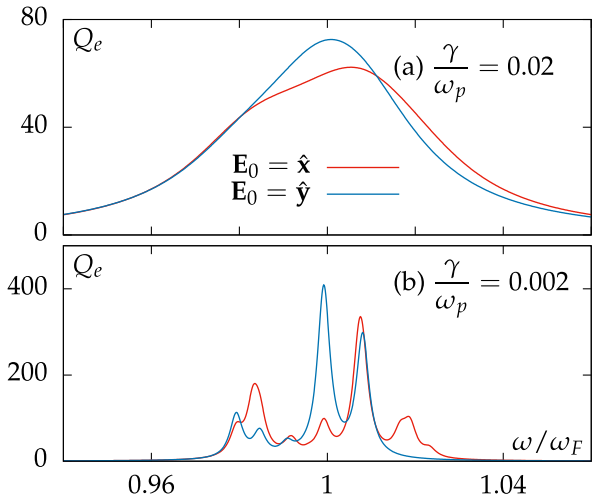

Fig. 5. Extinction spectra of the aggregate shown in Fig. 4 with $N=4$ elementary spheres for different ratios of γ/ω_p and different polarizations of the incident field. Spectra for the x and z polarizations coincide.

4. DISCUSSION

It is well known that the polarizability tensor $\hat{\alpha}$ is symmetric. In statics, this implies the existence of a rectangular reference frame XYZ in which $\hat{\alpha}$ is diagonal. If this was not so, we would have a good recipe for a perpetual motion machine. However, beyond statics, this argument does not apply. An oscillating electromagnetic field carries energy, which can be dissipated by a particle in various ways. Correspondingly, at finite frequencies, $\hat{\alpha}$ is, in general, complex symmetric. Properties of complex symmetric matrices are different from those of Hermitian or real symmetric matrices. In fact, any square matrix is similar to a complex symmetric matrix. Therefore, we are considering here algebraic objects of a very general form. The quasi-static polarizability is subject to some restrictions; in particular, its diagonal elements always have positive imaginary parts. It is an open question whether $\hat{\alpha}$ can be defective. Most likely, this

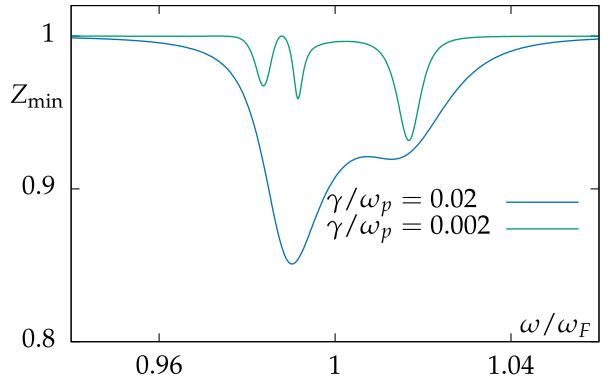

Fig. 6. Same as in Fig. 3 but for the aggregate shown in Fig. 4 with $N=4$.

Table 2. Same as in Table 1 but for the Aggregate Shown in Fig. 4[a]

Polarizability tensor $\hat{\alpha}$			
	x	y	z
x	(0.44, 1.08)	(-0.07, 0.11)	(-0.03, 0.01)
y	(-0.07, 0.11)	(0.58, 1.19)	(-0.07, 0.11)
z	(-0.03, 0.01)	(-0.07, 0.11)	(0.44, 1.08)
Eigenvalues α_p and eigenvectors $\mathbf{u}_p$			
	$p=1$	$p=2$	$p=3$
α_p	(0.40, 0.26)	(0.48, 1.07)	(0.59, 1.02)
u_{px}	(0.68, 0.00)	(-0.71, 0.00)	(-0.41, 0.25)
u_{py}	(0.35, 0.03)	(0.00, 0.00)	(0.73, 0.00)
u_{pz}	(0.44, 0.26)	(0.71, 0.00)	(-0.41, 0.25)
Pseudo-Euclidean orthogonality table, $\mathbf{u}_p \cdot \mathbf{u}_q$			
	$q=1$	$q=2$	$q=3$
$p=1$	(0.72, 0.47)	(0.00, 0.00)	(0.00, 0.00)
$p=2$	(0.00, 0.00)	(1.00, 0.00)	(0.00, 0.00)
$p=3$	(0.00, 0.00)	(0.00, 0.00)	(0.76, -0.41)

[a]Number of particles $N=4$. Other parameters: $\gamma/\omega_p=0.02$ and $\omega/\omega_F=0.98812$.

can happen, if at all, as a consequence of random (that is, not related to any symmetry) degeneracy in particles of complicated shape. However, even if $\hat{\alpha}$ is non-defective, its eigenvectors can be complex and not reducible to real vectors by multiplication with a constant.

In the remainder of this section, we discuss and summarize several relevant points.

A. Conditions

The most important condition for observing the effect described in this paper (that is, $\hat{\alpha}$ not having three real principal axes) is nonzero absorption. Particles made of a non-absorbing material with a purely real ϵ always have real principal axes regardless of the geometry. But complexity of ϵ is not enough. The particles should also lack symmetries, and some symmetries are not obvious. For example, the aggregate shown in Fig. 4 is not symmetric with respect to reflection in the plane $x+z=0$ or any of its parallel translations; however, $\hat{\alpha}$ for this aggregate has a real principal axis lying in that plane, $\mathbf{u}_2=(-\sqrt{2},\,0,\,\sqrt{2})$.

Additionally, interaction with the external field should be resonantly enhanced; the effect is absent in the first Born approximation. Accordingly, metals appear to be good candidates for materials in which the effect is present. However, the resonances should not be too narrow either; spectral overlap of several neighboring resonances is another condition for the effect to take place.

B. Generality

We have provided several examples of $\hat{\alpha}$ not having real principal axes using the coupled-dipole model. In constructing the examples, we made an effort to keep the dipole approximation accurate for the physical interpretation of the coupled dipoles as interacting metal spheres. We also made the point that this is not the only possible physical interpretation. However, the question whether the obtained results are specific to coupled dipoles was not answered directly. A general statement one can make is that the linear response of any continuous particle can be mimicked with arbitrary precision by a collection of point dipoles, although sometimes establishing the correspondence may be difficult. The coupled-dipole model therefore does not entail any loss of generality and, in particular, it does not violate any of the fundamental laws of electrodynamics.

We can also look at the question from a slightly different point of view. Instead of coupled dipoles, we could have started from the integral equation for the polarization field $\mathbf{P}(\mathbf{r})$, which is of the form

$$\kappa(\omega)\mathbf{P}(\mathbf{r}) = \frac{3}{4\pi}\left[\mathbf{E}_0 + \int_{\mathbb{V}} \hat{G}(\mathbf{r},\mathbf{r}')\mathbf{P}(\mathbf{r}')\mathrm{d}^3r'\right], \quad \mathbf{r}\in\mathbb{V}. \tag{18}$$

Here $\mathbb{V}$ is the spatial region occupied by the scatterer. Equation (18) is similar to the coupled-dipole equation in many important respects. We can introduce the integral operator $\mathbb{W}$ acting in the Hilbert space $\mathcal{H}(\mathbb{V})$ of square-integrable in $\mathbb{V}$ vector functions. The operator is real symmetric and has eigenvalues and eigenvectors w_n and $|\mathtt{P}_n\rangle$. In direct analogy to Eq. (16), we can write

$$\alpha_{pq}(\omega) = \frac{3}{4\pi}\sum_{n=1}^{N}\frac{\langle \mathtt{O}_p|\mathtt{P}_n\rangle\langle\mathtt{P}_n|\mathtt{O}_q\rangle}{\kappa(\omega)-w_n}, \tag{19}$$

where, for any $|\mathtt{f}\rangle\in\mathcal{H}(\mathbb{V})$,

$$\langle \mathtt{O}_p|\mathtt{f}\rangle = \int_{\mathbb{V}} f_p(\mathbf{r})\mathrm{d}^3r. \tag{20}$$

The only substantial difference between the spectral solutions (16) and (19) is that, in the latter equation, the summation is infinite and may include integration over a continuous spectrum. Another, less fundamental distinction is that it is much harder to compute the quantities w_n and $|\mathtt{P}_n\rangle$ for continuous particles numerically. The algebraic structure of the two solutions is however the same. The effect we are looking for occurs when $\kappa(\omega)$ is complex and several strong resonances defined by the equations $\mathrm{Re}[\kappa(\omega)] = w_n$ spectrally overlap.

C. Radiative Correction and Magnetic Polarizability

Excitation of the magnetic dipole and accounting for the radiative correction to the dipole polarizability are closely related. However, the effect described in this paper is different from accounting for a nonzero magnetic polarizability. Indeed, to obtain a nonvanishing magnetic moment, one must consider an incident field that is not strictly homogeneous but varies in space due to a finite wavelength. The electric dipole polarizability, in contrast, can be computed by assuming that the electric field is spatially uniform at any moment of time, i.e., given by $\mathrm{Re}[\mathbf{E}_0 e^{-\mathrm{i}\omega t}]$, where $\mathbf{E}_0$ is a constant amplitude. In a physical experiment, the particle under consideration may have both electric and magnetic dipole polarizabilities. The conclusions of this paper apply to the former. Note that the magnetic polarizability is not even a tensor.

Also, accounting for the radiative correction is important in computations involving scattering and energy budgets. However, the correction is proportional to the identity tensor and therefore does not affect the eigenvectors; it only shifts the imaginary parts of all three eigenvalues of $\hat{\alpha}$ by the same frequency-dependent amount.

Disclosures. The author declares no conflicts of interest.

Data availability. Data underlying the results presented in this paper are available in Dataset 1, Ref. [10].

REFERENCES

1. C. F. Bohren and D. R. Huffman, *Absorption and Scattering of Light by Small Particles* (Wiley, 1998).
2. B. Draine and P. Flatau, "Discrete-dipole approximation for scattering calculations," J. Opt. Soc. Am. A **11**, 1491–1499 (1994).
3. M. A. Yurkin and A. G. Hoekstra, "The discrete dipole approximation: an overview and recent developments," J. Quant. Spectrosc. Radiat. Transfer **106**, 558–589 (2007).
4. V. A. Markel, "Extinction, scattering and absorption of electromagnetic waves in the coupled-dipole approximation," J. Quant. Spectrosc. Radiat. Transfer **236**, 106611 (2019).
5. P. C. Chaumet, "The discrete dipole approximation: a review," Mathematics **10**, 3049 (2022).
6. V. A. Markel, *Extinction of Electromagnetic Waves*, Vol. **9** of Springer Series in Light Scattering (Springer, 2023), pp. 1–105.
7. H. Moosmüller, R. K. Chakrabarty, and W. P. Arnott, "Aerosol light absorption and its measurement: a review," J. Quant. Spectrosc. Radiat. Transfer **110**, 844–878 (2009).
8. B. D. Craven, "Complex symmetric matrices," J. Austral. Math. Soc. **10**, 341–354 (1967).
9. V. A. Markel, L. S. Muratov, and M. I. Stockman, "Optical properties of fractals: theory and numerical simulation," J. Exp. Theor. Phys. **71**, 455 (1990).
10. V. A. Markel, "Dataset for 'Does the quasi-static polarizability have principal axes?'," figshare (2024), https://doi.org/10.6084/m9.figshare.25374388.